www.czasopisma.pan.pl PAN POLSKA AKADEMIA NAUK www.journals.pan.pl
Chemical and Process Engineering 2017, 38 (3), 393-409
DOI: 10.1515/cpe-2017-0030

APPLICATION OF GAUSSIAN CUBATURE TO MODEL TWO-DIMENSIONAL POPULATION BALANCES

Jerzy Bałdyga[1], Grzegorz Tyl[*1], Mounir Bouaifi[2]

[1]Warsaw University of Technology, Department of Chemical and Process Engineering, Waryńskiego 1, 00-645 Warsaw, Poland

[2]Centre de Recherche et d'Innovation de Lyon, Solvay, 85 Avenue des Frères Perret, BP 62, 69192 Saint-Fons Cedex, France

In many systems of engineering interest the moment transformation of population balance is applied. One of the methods to solve the transformed population balance equations is the quadrature method of moments. It is based on the approximation of the density function in the source term by the Gaussian quadrature so that it preserves the moments of the original distribution. In this work we propose another method to be applied to the multivariate population problem in chemical engineering, namely a Gaussian cubature (GC) technique that applies linear programming for the approximation of the multivariate distribution. Examples of the application of the Gaussian cubature (GC) are presented for four processes typical for chemical engineering applications. The first and second ones are devoted to crystallization modeling with direction-dependent two-dimensional and three-dimensional growth rates, the third one represents drop dispersion accompanied by mass transfer in liquid-liquid dispersions and finally the fourth case regards the aggregation and sintering of particle populations.

Keywords: crystallization, drop breakage, extraction, Gaussian cubature, population balance, QMOM

1. INTRODUCTION

Multiphase reactors are very common in chemical industry and the population balance framework is considered as a pragmatic approach for modeling particulate, bubble or droplet dynamics in multiphase processes including polymerization, crystallization and precipitation systems. The last two processes i.e. crystallization and precipitation are used for more than 70% of solid materials produced by the chemical industry (Silva, 2007). Concerning industrial requirements it is preferred to have particles with high purity, desired size distribution, satisfactory stability and good shape. Producing a material with the desired quality often requires knowledge of the elementary steps involved in the process: creation of supersaturation, nucleation, particle growth, aggregation and other secondary processes. The product quality is mainly determined by operating conditions. However, these processes are still not well predictable because their course is strongly affected by complex interactions between fluid flow, mixing, particle aggregation and particle breakage subprocesses. Simple models are often used to interpret these effects but they do not account well for such complex interactions. To achieve real progress in an efficient process control and scale-up, a wide range of problems needs to be addressed by multidisciplinary, multiphysics and multiscale approaches – starting from the modeling of molecular level phenomena, to the crystal and, subsequently, the product design, including advanced measurement techniques coupled to advanced modeling tools. In order to properly model such complex

*Corresponding authors, e-mail: g.tyl@ichip.pw.edu.pl

phenomena, population balance equations supplemented with fast and efficient solution algorithms can be coupled with Computational Fluid Dynamics (CFD) modeling to correctly predict the particle size distribution (PSD).

One of the commonly used approaches for solving population balance equations in chemical engineering applications is the quadrature method of moments (QMOM), which has been introduced by McGraw (1997) to simulate the course of particulate processes. It is based on the approximation of the density function in the source term by the Gaussian quadrature so that it preserves the moments of the original distribution. In this method one determines weights and abscissas that are used in the quadrature approximation using inversion algorithms. McGraw (1997) applied the product-difference algorithm by Gordon (1968), although more such algorithms are available in the literature. One can mention the long quotient-modified difference algorithm from Sack and Donovan (1972) and the Golub-Welsch (1969) algorithm.

The Gaussian quadrature (GQ) approach generates the moment-preserving approximations for one-dimensional distributions. However, this feature does not generalize to multivariate probability distributions, with the exception of independent random variables.

Wright et al. (2001) extended the QMOM method to the multivariate population problem. As mentioned above, in this case no exact algorithms are available. Several attempts have been made to apply approximate algorithms also for the multidimensional case, which resulted for example in a multiple 3-point quadrature technique and a 12-point quadrature technique (Wright et al., 2001). The DQMOM equations (Marchisio and Fox, 2005) are derived via the moment transfer method, in a similar way to QMOM.

Currently there are no numerical techniques allowing to solve the closure problem generated by the moment transformation of population balance equations for the number of internal dimensions higher than two. In this work another method is proposed to be applied to the multivariate population problem in chemical engineering, namely a Gaussian cubature (GC) technique which applies linear programming for the approximation of the multivariate distribution. It can be applied to systems of an arbitrary number of internal dimensions without reformulation. This leads to simplicity of the solution method and shows universality of this approach. Gaussian cubatures are feasible for joint, but independent distributions. In spite of the fact that this method is heuristic for joint, dependent distributions, it appears to be reliable and to accurately approximate expectations of many functions. This approach has been used by DeVuyst and Preckel (2007) for the modeling of economic processes. Linear program returns weights (restricted to be positive) for each of the created lattice points. The maximum number of points with strictly positive weights is equal to the number of constraints used.

Examples of the application of the Gaussian cubature (GC) are presented in this paper for four processes typical for chemical engineering applications. The first and second cases are devoted to crystallization modeling with direction-dependent growth rates. The third one represents drop dispersion accompanied by mass transfer in liquid-liquid dispersions, and in the fourth case the aggregation and sintering of particle populations is considered. In the first, third and fourth cases, two-dimensional population balance equations (PBE) are used. In the second case a 3-dimensional crystal growth in the MSMPR crystallizer is simulated to show the possibility of the proposed numerical scheme to address the cases with more internal dimensions.

2. THE METHOD OF MOMENTS APPROACH FOR SOLVING POPULATION BALANCE EQUATIONS

The population balance equations are powerful tools that are used to predict the behavior of dispersed systems. For the first time they were introduced by Hulburt and Katz (1964) and emerged from the

dynamic description of a dispersed system treated as a statistical ensemble moving through the phase space. This statistical mechanical approach resulted in the system of integro-differential equations (Eq. (1)) governing the evolution of the distribution f, of dispersed phase properties in a way similar to the Liouville theorem of classical statistical mechanics (Sorgato, 1981; Hulburt and Katz, 1964).

$$\frac{\partial f}{\partial t}+\sum_{i=1}^{3}\frac{\partial\left\{v_i\left(\boldsymbol{x},t\right)f\right\}}{\partial x_i}+\sum_{j}^{N}\frac{\partial\left\{G_j f\right\}}{\partial r_j}=B\left(\boldsymbol{x},\boldsymbol{r},t\right)-D\left(\boldsymbol{x},\boldsymbol{r},t\right) \tag{1}$$

The phase space consists of external coordinates, $\boldsymbol{x}$, describing the position of particles in the physical space and internal coordinates, $\boldsymbol{r}$, that characterize properties of the dispersed phase, i.e. the size of particles or droplets, species concentration within droplets, fractal dimension of aggregates and many other. The convective flow of points through the phase space is described by the velocities v_i in the physical space, and G_j in the space of internal coordinates, which can be physically interpreted as the growth rate of crystals or dissolution of liquid droplets depending on the system under consideration. Also new points can appear or disappear in the phase space corresponding to effects of breakage or coalescence of droplets, as well as aggregation and breakage of solid crystals. Those effects are defined by the birth and death functions, $B(\boldsymbol{x},\boldsymbol{r},t)$ and $D(\boldsymbol{x},\boldsymbol{r},t)$. Although the population balance equations are well defined, they are difficult to solve due to high dimensionality of the system, especially when nonlinear source terms are present. For linear cases, Hulburt and Katz (1964) introduced the method of moments which allowed to transform the set of partial differential equations into the set of ordinary differential equations and reduce the dimensionality of the system. The transformed set of population balance equations is easier to solve. However, instead of the full distribution of the dispersed phase properties one gets only average values defined by the moments of distribution:

$$m_{k_1,k_2,\ldots,k_N}=\int_0^\infty\int_0^\infty\ldots\int_0^\infty r_1^{k_1}r_2^{k_2}\ldots r_N^{k_N}f\left(\boldsymbol{r},t\right)dr_1dr_2\ldots dr_N \tag{2}$$

The expected values of distribution can describe many physical properties of the dispersed phase like the number of particles, average size, area or volume. The set of the ordinary differential equations for the moments is generated by the moment transformation as given below:

$$\begin{aligned}\int_0^\infty\int_0^\infty\ldots\int_0^\infty r_1^{k_1}r_2^{k_2}\ldots r_N^{k_N}\left(\frac{\partial f}{\partial t}+\sum_{i=1}^{3}\frac{\partial\left\{v_i\left(\boldsymbol{x},t\right)f\right\}}{\partial x_i}+\sum_{j}^{N}\frac{\partial\left\{G_j f\right\}}{\partial r_j}\right)dr_1dr_2\ldots dr_N=\\ =\int_0^\infty\int_0^\infty\ldots\int_0^\infty r_1^{k_1}r_2^{k_2}\ldots r_N^{k_N}\left(B\left(\boldsymbol{x},\boldsymbol{r},t\right)-D(\boldsymbol{x},\boldsymbol{r},t)\right)dr_1dr_2\ldots dr_N\end{aligned} \tag{3}$$

In many cases the birth and death functions consist of nonlinear terms, a good example here is aggregation. In such cases the moment transformation creates the closure problem, i.e. the set of equations becomes unclosed as there are more unknowns than equations. The closure problem can be solved by introducing some additional information. For systems with one internal dimension this can be done by using the quadrature method of moments (QMOM) introduced by McGraw (1997). It applies a quadrature approximation of the source term integrals using so called inversion algorithms such as a product-difference (PD) algorithm (Gordon, 1968). QMOM has been further generalized to bivariate cases (Wright et al., 2001) i.e. where two internal coordinates are used to describe the dispersed phase system. In the current state of the art there are no numerical techniques allowing to solve without approximation the closure problem generated by the moment transformation of population balance equations for the number of internal dimensions higher than two. Therefore another efficient approximate method, the Gaussian Cubature (GC) numerical scheme, has been developed to approach the closure problem in multidimensional cases for an arbitrary number of internal coordinates.

3. GAUSSIAN CUBATURE TECHNIQUE

The introduced technique is based on the approximation of the source term integrals in the moment - transformed PBEs by a Gaussian cubature, such that:

$$E\left[g\left(\boldsymbol{X}\right)\right]=\int g\left(\boldsymbol{X}\right)f\left(\boldsymbol{X}\right)d\boldsymbol{X}\approx\sum_{i=1}^{N}g\left(\boldsymbol{X}_i\right)w_i \tag{4}$$

where $\boldsymbol{X}$ is an s-dimensional vector of random variables having density $f(\boldsymbol{X})$, and $g(\boldsymbol{X})$ denotes the integrand function i.e. function whose expected value is to be computed.

To apply this approximation it is necessary to determine weights w_i, and abscissas $\boldsymbol{X}_i$ of the cubature points. GC technique chooses points and weights for the cubature approximation so as to preserve the lower-order moments of the original distribution. A d-degree GC approximation can be defined by the following system of linear equations:

$$\sum_{i=1}^{N}w_i\prod_{j=1}^{s}\left(x_{ij}\right)^{k_j}=E\left[\prod_{j=1}^{s}\left(X_j\right)^{k_j}\right] \tag{5}$$

with

$$\sum_{j=1}^{s}k_j\le d,k_j\ge 0,w_i\ge 0 \tag{6}$$

By E the expectation value is denoted, hence the right-hand sides of Equation (5) are the raw moments of order at most d of the approximated distribution.

To determine weights and abscissas of the cubature points it is necessary to set up a lattice in s-dimensional domain. It is done by following the algorithm presented by DeVuyst and Preckel (2007). First an equally spaced grid over each variable is set up. The range of each variable has to be chosen based on the knowledge of the process conditions. The number of created grid points is an important parameter that determines the convergence of the algorithm (more points to choose from) but also sufficiently influences calculation time, so it has to be chosen as low as possible but large enough to ensure determination of the cubature points. The lattice in s-dimensional phase space is formed by a Cartesian product of the previously created grids over each axis.

The second step is to set up a linear program (LP) over the lattice points using the system expressed by Eq. (5) as the equality constraints. Because one is interested in obtaining any set of points having positive weights that satisfy Eq. (5), the objective function vector is set to zero. The LP can be solved via Simplex method, which results in a set of weights associated to vectors of the feasible basis. Each of those vectors corresponds to the specific point in the phase space resulting in a complete set of points with associated weights for the cubature approximation.

During iterative solving of population balance equations the GC is calculated in each time step and then used to determine integrals in the source term. It occurred that during the time evolution of the initial distribution, the above presented algorithm could not find a feasible solution even for a dense lattice. Therefore some changes have been introduced to the algorithm to assure better convergence. The most important modification is the exchange of the set of equality constraints, Eq. (5), for the set of inequality constraints defined as follows:

$$\sum_{i=1}^{N}w_i\prod_{j=1}^{s}\left(x_{ij}\right)^{k_j}\le E\left[\prod_{j=1}^{s}\left(X_j\right)^{k_j}\right]\cdot\left(1+Tol\right) \tag{7}$$

$$\sum_{i=1}^{N} w_i \prod_{j=1}^{s} \left(x_{ij}\right)^{k_j} \geq E\left[\prod_{j=1}^{s} \left(X_j\right)^{k_j}\right] \cdot \left(1 - Tol\right) \tag{8}$$

In the above set, *Tol* denotes the tolerance of moments determination by the linear program. Introducing this parameter enables one to control the desired accuracy but also for some cases allows the LP to find a feasible solution. This modification also makes it easy to find the initial feasible basis for the linear programming solver. The initial basis consisting of vectors corresponding to the slack variables is in this case dual-feasible, hence the dual-simplex algorithm is further used to solve the LP.

To demonstrate the possibilities of the above introduced algorithm, four test cases are presented in the following sections. The first one regards the seeded crystallization process including the nucleation and growth of crystals in two directions (2D growth). Then a 3-dimensional population balance model of crystal growth and nucleation will be presented, showing the possibility of applying the above presented numerical scheme. The third test case is the extraction process in a water-acetone-toluene system. Bivariate population balance is used to simulate the simultaneous drop breakage and mass transfer in the system. In the last test case the aggregation and sintering of the population of particles is considered, which has been also approached by Wright et al. (2001) when introducing the bivariate extension of the QMOM technique. PBEs are solved using MATLAB programming language and the dual-simplex algorithm implemented in the software.

4. APPLICATION OF GC TO CRYSTALLIZATION PROCESS

4.1. 2D case

As the first test case for the presented method the two-dimensional population balance model of the pharmaceutical crystallization process (Sen et al., 2014) has been chosen. Sen et al. (2014) developed a model for the growth of crystals in two dimensions. Model constants for the kinetics of the process have been also determined. The population balance equation describing this process takes the form:

$$\frac{\partial f\left(L_1, L_2, t\right)}{\partial t} + \frac{\partial\left(G_1\left(L_1, t\right) f\left(L_1, L_2, t\right)\right)}{\partial L_1} + \frac{\partial\left(G_2\left(L_2, t\right) f\left(L_1, L_2, t\right)\right)}{\partial L_2} = B_0\left(C, t\right)\delta\left(L_1\right)\delta\left(L_2\right) \tag{9}$$

Where G_1 and G_2 denote the rate of crystal growth in directions L_1 and L_2 respectively and B_0 stands for the rate of nucleation. The growth rates can be written as follows (Gunawan et al., 2004):

$$G_1 = k_{g1}\left(\frac{C - C_{sat}}{C_{sat}}\right)^{g_1} \tag{10}$$

$$G_2 = k_{g2}\left(\frac{C - C_{sat}}{C_{sat}}\right)^{g_2} \tag{11}$$

In this model only secondary nucleation is taken into account and its rate is given by:

$$B_0 = k_b S\left(L_1, L_2, t\right)\left(\frac{C - C_{sat}}{C_{sat}}\right)^{bs} \tag{12}$$

Kinetic constants: k_{g1}, k_{g2}, k_b, g_1, g_2, have been determined by Sen et al. (2014) by fitting them to experimental data. In the above equation C stands for the concentration of the solute and C_{sat} denotes the solubility of the solute. Since it is assumed that the shape of crystals is cuboid with two

characteristic dimensions L_1 and L_2, the surface area of the single crystal is $2L_1^2 + 4L_1L_2$, which after integration over the whole population results in the total surface area of the crystals S(L_1, L_2, t):

$$S(L_1,L_2,t) = \int_0^\infty\int_0^\infty F(L_1,L_2,t)\left(2L_1^2 + 4L_1L_2\right)dL_1dL_2 \tag{13}$$

The above presented model has to be solved simultaneously with the mass balance in the form:

$$\frac{dC}{dt} = -\rho_c \int_0^\infty\int_0^\infty F(L_1,L_2,t)\left(2G_1\left(L_1L_2 - L_1^2\right) + G_2L_1^2\right)dL_1dL_2 \tag{14}$$

where ρ_c stands for the density of crystals.

The described crystallization process is a cooling process so the nucleation and growth of crystals are caused by the decrease in solute solubility with decreasing temperature. For the test case of our GC technique, linear solubility change in time has been used (data set 1.1 from Sen et al. (2014)). The density of crystals has been assumed by us to be ρ_c = 1500 kg/m^3. Moment transformation of (9) results in the system of ordinary differential equations for the lower-order moments of crystal size distribution. There is no closure needed in the model, hence it can be solved explicitly and therefore is the perfect base for comparison to the introduced GC technique. The parameters chosen to be compared for this process are the characteristic length and aspect ratio defined as follows:

$$D_{avg} = \left(\overline{L_1L_2^2}\right)^{1/3} \tag{15}$$

$$AR = \frac{\bar{L}_1}{\bar{L}_2} \tag{16}$$

Calculations were made using cubature of degrees 3 and 5. In this case they both gave exactly the same results because only moments of order equal of less than 3 were needed to calculate D_{avg} and AR.

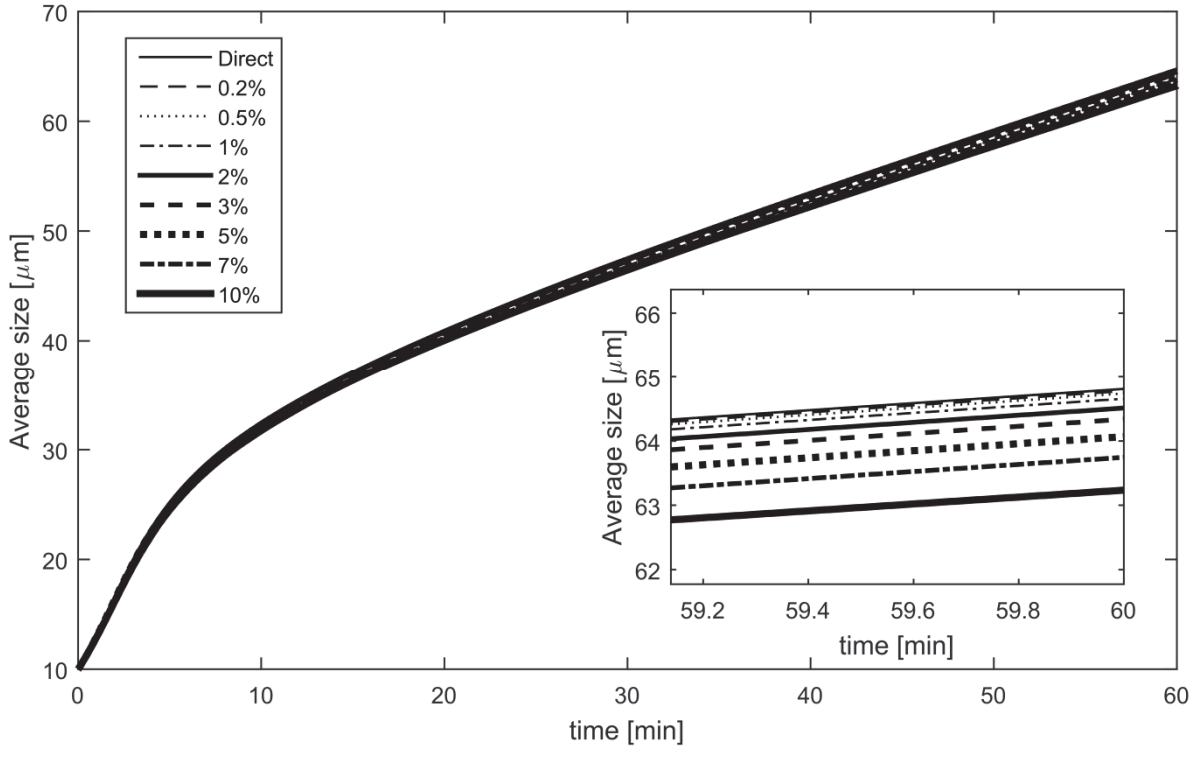

Fig. 1. Comparison of calculated crystal average size for different cubature tolerance with results of direct solution

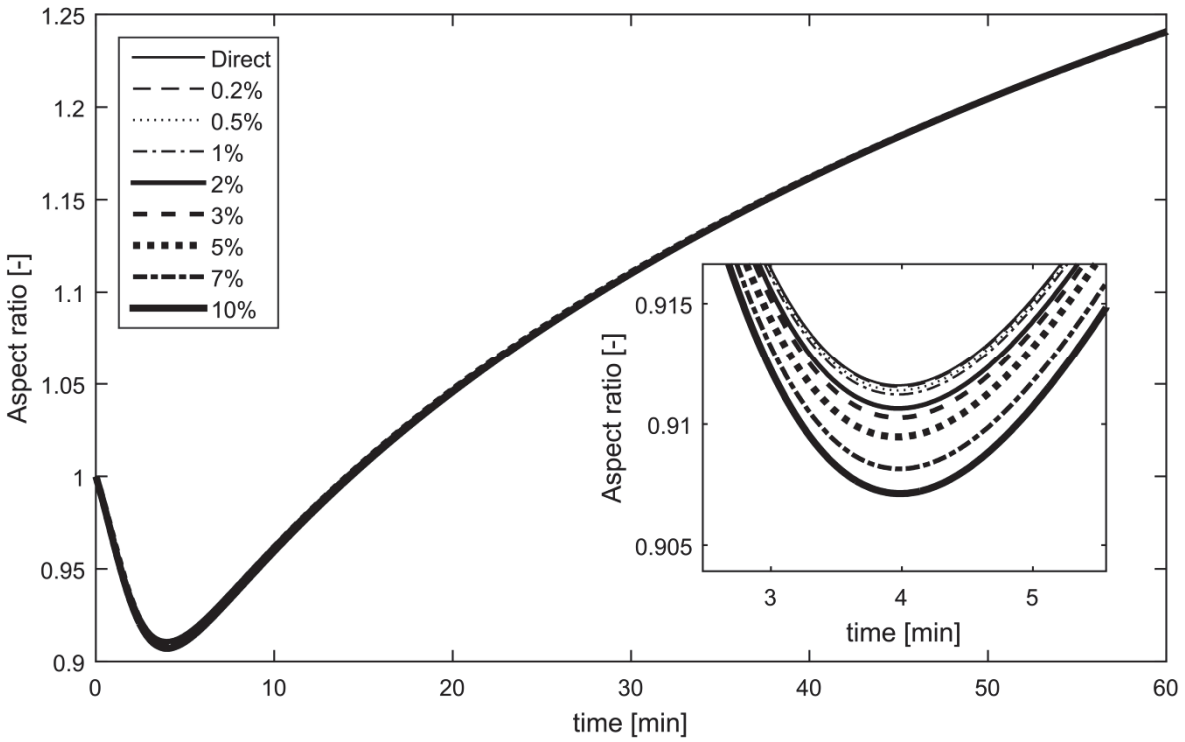

Fig. 2. Comparison of aspect ratio for different cubature tolerances with results of direct solution

Table 1. Percent error of characteristic size and aspect ratio determination

Tolerance	Final average size [μm]	Error [%]	Final Aspect Ratio	Error [%]
Direct	64.810	0.000	1.2399	0.000
0.20%	64.776	-0.052	1.2399	0.000
0.5%	64.737	-0.113	1.2399	0.000
1%	64.657	-0.236	1.2401	0.016
2%	64.511	-0.461	1.2401	0.016
3%	64.337	-0.730	1.2401	0.016
5%	64.067	-1.146	1.2405	0.048
7%	63.746	-1.642	1.2401	0.016
10%	63.235	-2.430	1.2407	0.065

In Figs. 1 and 2 time dependencies of those parameters are presented. It can be noticed that increasing the cubature tolerance only slightly influences the calculated final crystal size but has almost no influence on the final aspect ratio. The relative error of average size and aspect ratio determination is presented in Table 1.

An important factor influencing the calculation time and the minimum possible tolerance is the number of divisions of each axis. Increasing the number of points along each axis enables to decrease the cubature tolerance but also sufficiently influences calculation time due to the significant rise in the number of lattice points. Calculation time of 6000 time steps is presented in Table 2. It can be noticed that for a certain number of domain divisions there exists a minimum achievable tolerance where the linear program solver can still find a feasible solution in each time step. Execution time generally does not depend on the cubature tolerance but for some reason for 20 axis divisions and 7% tolerance it calculates two times faster. A similar minimum seems to exist for 50 axis divisions and 1% tolerance.

The tolerance of 0.2% can be achieved with 80 axis divisions but it also results in the increase in execution time of up to around 1200s.

Table 2. Calculation time in seconds of 6000 time steps depending on cubature tolerance and number of axis divisions (Intel Core i7-2630QM 2GHz, 8GB DDR3)

Tolerance	Number of axis divisions		
	10	20	50
10%	589	581	787
7%	-	296	818
5%	-	598	807
3%	-	561	817
2%	-	-	833
1%	-	-	659
0.5%	-	-	872

4.2. 3D case

The crystal growth case can be extended to the 3D model if one needs to consider the independent growth of each crystal face. The natural extension is the growth model of 3D cuboid shaped crystals. As an example a process taking place in the MSMPR continuous crystallizer is considered. The process kinetics has been taken from Borchert et al. (2009). In this paper the authors considered a system in the steady state and checked the influence of the mean residence time on crystal dimensions. In the present work a dynamic model has been developed and solved using GC to check if it converges to the steady state results presented in the paper by Borchert et al. (2009). Similarly as in the previous test case the model equations were solved directly to have the dynamic results for comparison. A cuboid shape of crytals has been assumed with crystal dimensions, h_1, h_2, h_3, measured from the center. For the simulation the following set of moments of crystal size distribution: $m_{0,0,0}$, $m_{1,0,0}$, $m_{0,1,0}$, $m_{0,0,1}$, $m_{1,1,1}$, $m_{2,0,0}$, $m_{0,2,0}$, $m_{0,0,2}$, $m_{1,1,0}$, $m_{1,0,1}$, $m_{0,1,1}$ was used. This is equivalent to the GC of degree 2 with the additional moment $m_{1,1,1}$ that is present in the mass balance and therefore has to be accurately determined to minimize the error. After performing the moment transformation of the population balance equations one gets the following set of governing equations for the moments of crystal size distribution in the crytalizer having mean residence time θ:

$$\frac{dm_{0,0,0}}{dt} = B_0 - \frac{m_{0,0,0}}{\theta} \tag{17}$$

$$\frac{dm_{k,l,n}}{dt} = kG_1 m_{k-1,l,n} + lG_2 m_{k,l-1,n} + nG_3 m_{k,l,n-1} - \frac{1}{\theta} m_{k,l,n} \tag{18}$$

where G_1, G_2, G_3 are the face specific growth rates given by:

$$G_i = k_{g,i}\sigma^{g_i} \tag{19}$$

Kinetic constants $k_{g,i}$ and g_i are taken directly from the paper by Borchert et al. (2009) and the supersaturation is defined as follows:

$$\sigma = \frac{C - C_{sat}}{C_{sat}} \tag{20}$$

where C is the mass concentration of the solute and C_{sat} denotes the saturation concentration.

The rate of nucleation, B_0, is assumed to be a power law dependency:

$$B_0 = k_b \sigma^b \tag{21}$$

It should be noted that the system parameters in the paper by Borchert et al. (2009) do not refer to a specific physical system.

Simultaneously to the population balance equations, the mass balance given by Eq. (22) has been solved.

$$\frac{dC}{dt} = \frac{1}{\theta}\left(C_{in} - C\right) - 8\rho_s \left(\frac{dm_{1,1,1}}{dt}\right)_{kin} \tag{22}$$

Where ρ_s denotes the solid density. The first term on the right-hand side of Eq. (22) describes the net flux of the solute to the system. The second term represents the decrease of solute concentration due to crystallization. Subscript *kin* denotes the first three terms on the right-hand side of Eq. (18) that describe the concentration drop described by the crystal growth kinetics. These three terms of Eq. (18) are substituted to Eq. (22) for *k, l, m* = 1.

The considered system has been simulated for two mean residence time values, $\theta = 0.36$ s and $\theta = 1$ s, which correspond to the characteristic points predicted by the steady state model. As the initial condition a supersaturated state was assumed with the inlet and outlet solutions having equal supersaturation, $\sigma_0 = \sigma_{in} = 2$. In Fig. 3. the evolutions of the characteristic crystal dimensions obtained using GC and by direct calculation are presented depending on the mean residence time in the crystallizer. In the first case (Fig. 3a)) the needle-like shape of the crystals is observed, which also corresponds to the result presented by Borchert et al. (2009). In the second case (Fig. 3b)) the cubic crystal shape is predicted, which also was obtained by the steady state model. The cubature tolerances used in those cases were 0.01 and 0.02 respectively. For both accuracy levels the results do not differ much from results of the direct solution of the PB. The comparison of relative error obtained using GC approximation is presented in Table. 3. One can see that while for the crystal dimensions the relative error is of the order of a few percent, for supersaturation it is actually negligible even for the higher tolerance. The evolution of supersaturation in time is virtually identical for both numerical methods (see Fig. 4.).

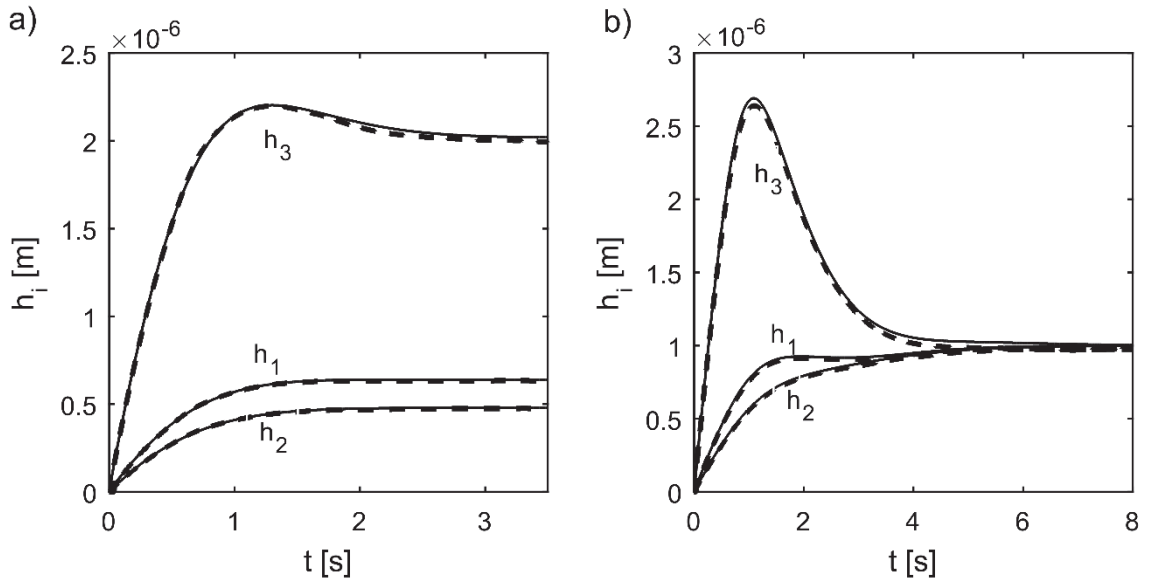

Fig. 3. Time evolution of the characteristic crystal dimensions for different mean residence times (direct solution - solid line, GC - dashed line); a) $\theta = 0.36$ s, b) $\theta = 1$ s

Table 3. Relative error of determining the steady state values using GC approximation for the considered cases

	$\theta = 0.36$ s			$\theta = 1$ s		
	Direct	Cubature	Error [%]	Direct	Cubature	Error [%]
h_1 [m]	6.40E-07	6.31E-07	1.41	1.00E-06	9.63E-07	3.73
h_2 [m]	4.80E-07	4.73E-07	1.42	1.00E-06	9.63E-07	3.68
h_3 [m]	2.02E-06	1.99E-06	1.35	1.00E-06	9.60E-07	4.01
σ [-]	1.7768	1.7765	0.02	1.0000	0.9989	0.11

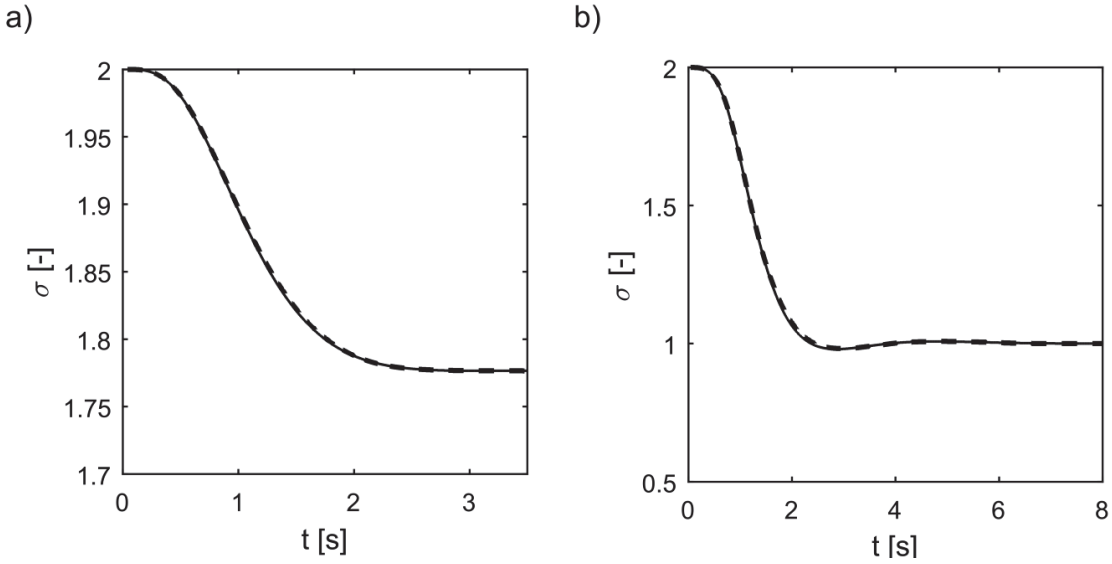

Fig. 4. Evolution of the supersaturation in the crystallizer predicted using GC and direct method for a) $\theta = 0.36$ s, b) $\theta = 1$ s (direct method - solid line, GC - dashed line)

5. APPLICATION OF GC TO MODELING OF MASS TRANSFER IN LIQUID - LIQUID SYSTEMS

For the full description of some processes like extraction or absorption it is necessary to follow not only the dispersed phase size distribution but also concentration of the extracted/absorbed component in both phases. The system under investigation is water-benzoic acid-toluene with water as the continuous phase, toluene as the dispersed phase and benzoic acid as the component transferred between phases. The dispersion is mixed in a 10 dm^3 stirred tank (diameter, $T = 0.23$ m, height, $H = 0.24$ m) equipped with a 0.133 m diameter Rushton turbine.

For the modeling the two-cell model introduced by Okamoto (1981) is applied. Population balance equations are solved using GC technique and compared with results obtained using bivariate quadrature method of moments with a 3-point quadrature technique for the approximation of weights and abscissas. In QMOM diameter is chosen to be the main coordinate on which the process depends, therefore abscissas on the size axis are first calculated from the moments of distribution with respect to diameter using product-difference algorithm and then concentrations are calculated from the mixed moments $m_{3,1}$, $m_{4,1}$, $m_{5,1}$ which define a linear system of equations.

The partition coefficient of the benzoic acid has been calculated from the formulas proposed by Brändström (1966):

$$\frac{C_{BT}}{C_{HBW}} = 1.09 + 1.009 C_{HBW} \tag{23}$$

where C_{BT} is the total concentration of benzoic acid in toluene and C_{HBW} is the concentration of not dissociated benzoic acid in water. The mass transfer coefficient introduced by Batchelor (1980) has been used with diffusion coefficient of the benzoic acid in water in 20 °C equal to $D = 0.91\times10^{-9}$ m^{2}s^{-1}. Driving force of the mass transfer process is:

$$\Delta C = \langle C_{bulk} \rangle - C_{HBW} \tag{24}$$

Where C_{HBW} is the concentration of the benzoic acid in water which would be in the equilibrium state with C_{BT} concentration in the dispersed phase so it directly depends on the droplet composition. The mean concentration of acid in the bulk $\langle C_{bulk} \rangle$ is calculated from the mass balance of the transferred component in the form:

$$V \cdot \phi \cdot \left(\langle C_d \rangle_0 - \langle C_d \rangle \right) = V \cdot (1-\phi) \cdot \left(\langle C_{bulk} \rangle - \langle C_{bulk} \rangle_0 \right) \tag{25}$$

which gives:

$$\langle C_{bulk} \rangle = \langle C_{bulk} \rangle_0 + \frac{\phi}{1-\phi} \left(\langle C_d \rangle_0 - \langle C_d \rangle \right) \tag{26}$$

It should be noted that in this case there are no direct solutions and the methods based on approximation have to be used. In the comparison of QMOM and GC model predictions, toluene is assumed to be the dispersed phase. Benzoic acid is initially present only in the droplets and transfers to the bulk during the process. In the calculations dispersed phase concentration $\phi = 10\%$ is used. Average energy dissipation rate in the tank is assumed to be $\varepsilon = 5$ W/kg.

The applied model consists of breakage kernel developed by Bałdyga and Podgórska (1998) based on the multifractal model of intermittency described in detail by Bałdyga and Bourne (1993, 1995). The continuous parabolic daughter size distribution introduced by Hill (1995) has been used.

In Figs. 5 and 6 predicted mean drop diameters are presented. Results obtained using the introduced GC technique are in agreement with QMOM predictions for d_{10} as well as for Sauter diameter d_{32}. Time dependence of the mean concentration of benzoic acid in the dispersed phase is presented in Fig. 7. In this case GC technique gives the same prediction as the QMOM. Details regarding the application of GC algorithm to modeling of mass transfer in liquid-liquid dispersions are presented in Appendix.

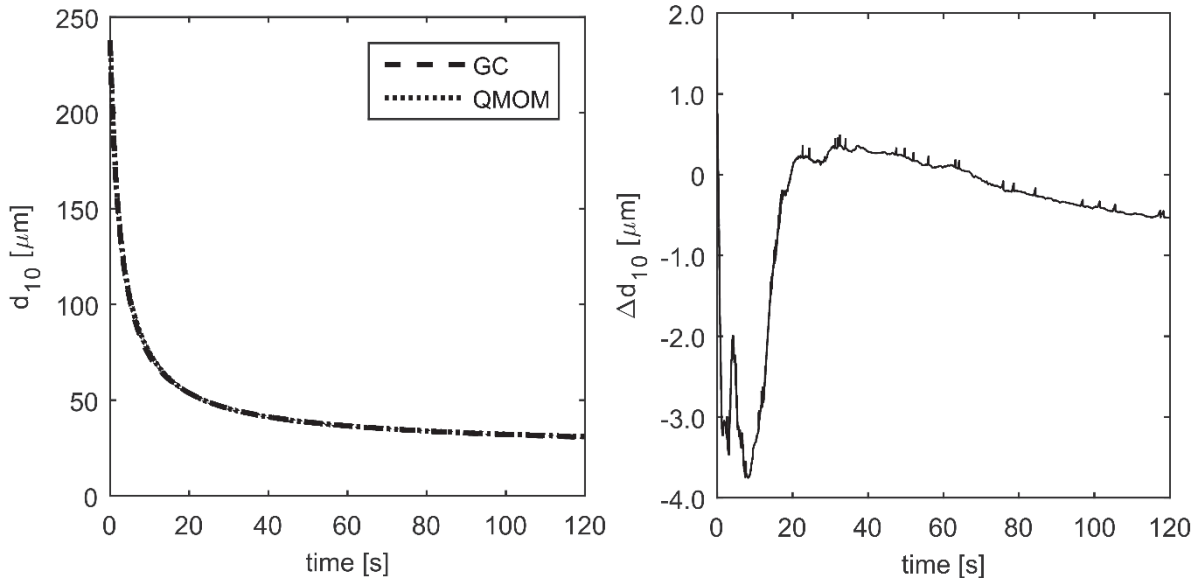

Fig. 5. Comparison of mean drop size d_{10} calculated using GC and QMOM. Δd_{10} denotes the difference between the results obtained using GC and QMOM techniques

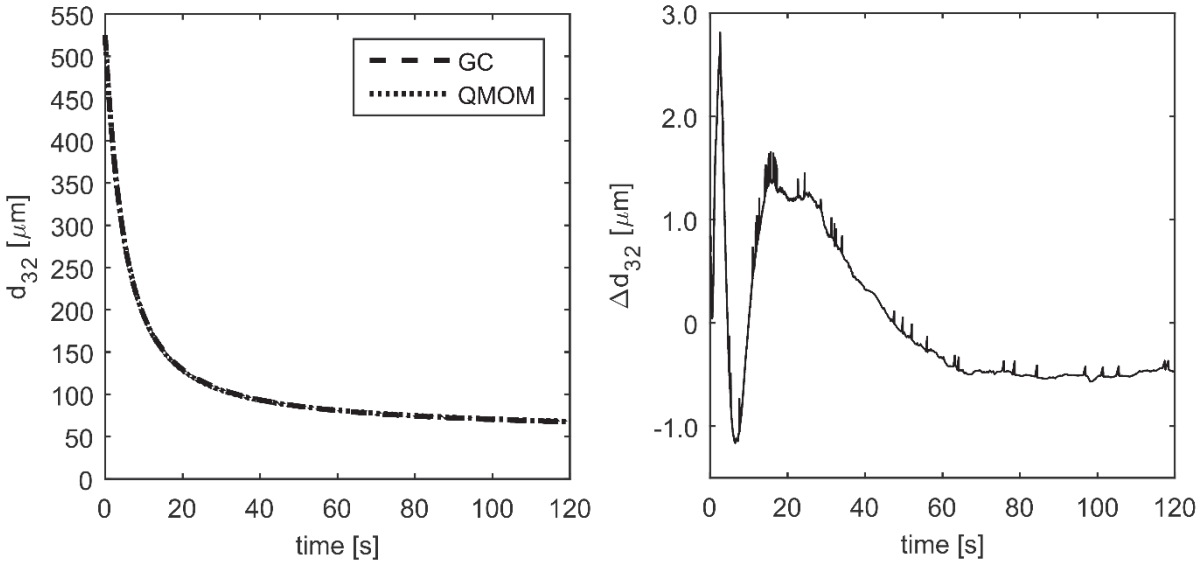

Fig. 6. Comparison of droplet Sauter diameter d_{32} calculated using GC and QMOM. Δd_{32} denotes the difference between the results obtained using GC and QMOM techniques

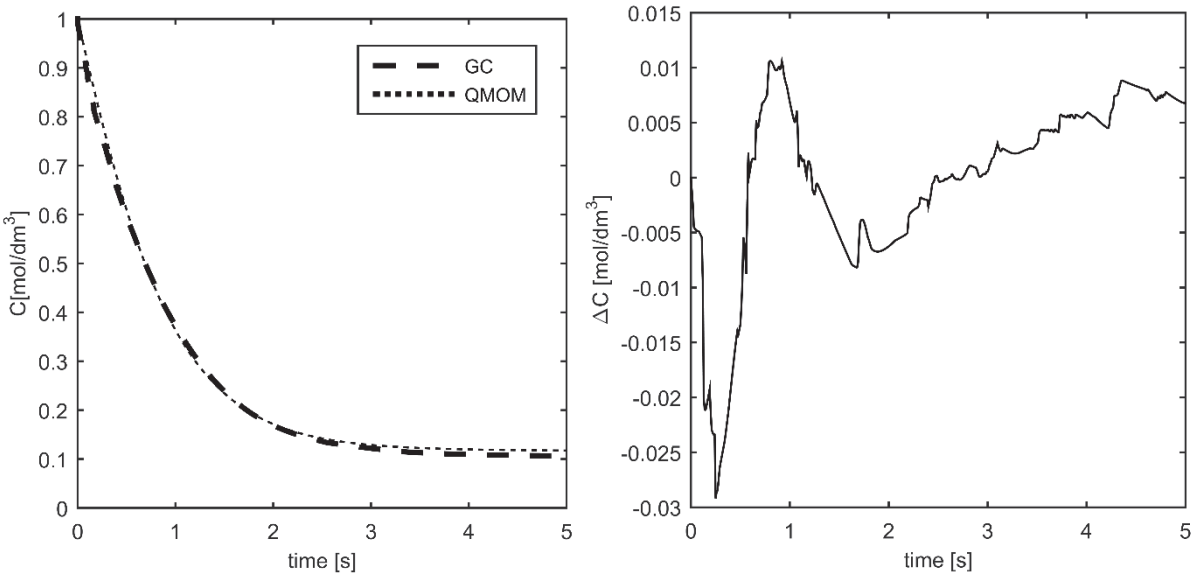

Fig. 7. Evolution of the mean concentration of benzoic acid in the dispersed phase. ΔC denotes the difference between the results obtained using GC and QMOM techniques

6. APPLICATION OF GC TO MODELING OF AGGREGATION AND SINTERING OF SOLID PARTICLES

The last test case regards the 2-dimensional model of aggregation and sintering of particle populations considered earlier by Wright et al. (2001). Aggregation is modeled by the Brownian coagulation kernel (Eq. 27) and the sintering by the convection in the phase space using relaxation term (Eq. 28).

$$\beta\left(V_1,V_2\right)=K\cdot\left(V_1^{-1/D_f}+V_2^{-1/D_f}\right)\left(V_1^{1/D_f}+V_2^{1/D_f}\right) \tag{27}$$

$$\left[\frac{\partial f\left(V_p,a\right)}{\partial t}\right]_{sint} = -\frac{\partial}{\partial a}\left[\dot{a}f\left(V_p,a\right)\right] \tag{28}$$

with

$$\dot{a} = -\frac{1}{t_f}\left(a - a_{min}\right) \tag{29}$$

where a_{min} is the area of a fully compacted (spherical) particle and t_f is the characteristic time of sintering. In this case we have assumed $t_f = 10$ s, $K = 1$ m^3/s, and $D_f = 3$ after McGraw et al. (2001). The initial distribution was lognormal over each axis with the initial moments taken directly from the paper.

Due to the presence of nonlinear terms in the PB equations the closure problem is generated by the moment transformation. The model has been solved using GC and two variants of bivariate QMOM for comparison. Both of them are 3 point bivariate quadrature techniques. QMOM(v) has volume chosen to be the primary variable. It means that first the monovariate quadrature is calculated from pure volume moments and then the corresponding specific areas are recalculated from moments of order 1/3 over the area. QMOM(a) is constructed similarly using the area as the primary variable. They are less exact than the complete 12p QMOM but much faster.

In GC the moments of the order up to 2 were followed, plus the 1/3 and -1/3 moments over the volume coordinate due to their presence in the aggregation kernel. 50 axis divisions and 0.1% tolerance have been used. The calculation time was 12.15 s/1000 time steps for the QMOM techniques and 79.6 s/1000 time steps for GC. We can see that the QMOM is faster but the more accurate techniques like 12p QMOM are about 100 times slower than QMOM as stated by the authors. For 12p QMOM we would also need to follow 36 moments of the distribution compared to 7 moments needed for the GC.

In Fig. 8 the time changes of average volume and average surface area of the particles are presented. We can see that the GC can predict accurately the effect of aggregation as well as sintering. QMOM(v) results for the area differ from the others when predicting surface area and QMOM(a) predicts aggregation effect less accurately.

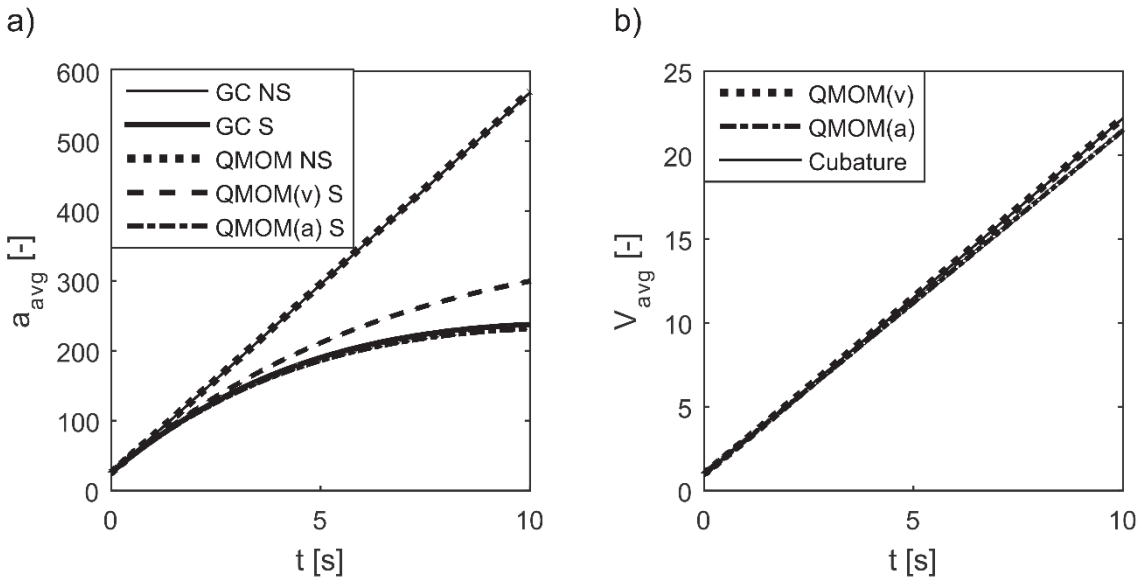

Fig. 8. Time evolution of a) average surface area, b) average volume of the particle population (NS - without sintering, S - with sintering)

7. CONCLUSIONS

A new moment based method for solving multidimensional population balance has been applied to chemical engineering processes. This new approach uses linear programming algorithms to develop a Gaussian cubature approximation of multivariate distributions which is further used to solve PBEs. The method has been applied to bivariate and 3-dimensional population balances, and proved to accurately describe the evolution of systems under investigation. Therefore it can be considered as a promising technique for the future implementation in CFD codes. Compared to other methods like QMOM the presented algorithm has no limitations in the number of internal dimensions and therefore it can be used to precisely determine the evolution of many independent parameters of the system under consideration. Also, the algorithm itself does not require any reformulation before being applied to higher dimensional systems, which makes it convenient to use. However, there are two parameters to be adjusted by the user, which severely influences the performance of this numerical scheme. From those two i.e. the grid resolution and cubature tolerance the latter seems to be more important for the overall performance while keeping the grid density in reasonable range (between 20 and 50 divisions of each axis). The tolerance influences the convergence of the algorithm and its precision. To overcome the problem of lack of convergence at some points in simulations, which would cause the crash of the program, the authors suggest using a loop, which in each time step starts the cubature with low tolerance. In the case of no convergence the tolerance should be subsequently increased to the level which allows for convergence. For simulations of higher dimensional systems another problem may arise, namely a significant increase in the number of lattice points with the rising number of axis divisions. In those cases it would be necessary to decrease the number of axis divisions at the cost of increasing the tolerance to keep the execution time reasonable. Those issues will have to be addressed before implementing the GC algorithm in the CFD code to ensure the stability and convergence of the simulation.

The authors gratefully acknowledge the financial support from Solvay, France.

SYMBOLS

a	dimensionless surface area of the particle
a_{avg}	dimensionless average surface area of the population of particles
a_{min}	dimensionless area of the fully compacted particle
AR	aspect ratio
$B(\mathbf{x}, \mathbf{r}, t)$	birth function
B_0	nucleation rate, $m^{-3}s^{-1}$
C	concentration of solute, kg/m^3
C_{bulk}	concentration of benzoic acid in water phase, mol/dm^3
C_{BT}	equilibrium concentration of benzoic acid in toluene, mol/dm^3
C_d	concentration of benzoic acid in toluene phase, mol/dm^3
C_{HBW}	equilibrium concentration of benzoic acid in water, mol/dm^3
C_{sat}	saturation concentration, kg/m^3
d	degree of GC approximation
d_d	droplet diameter, μm
d_{10}	average droplet size, μm
d_{32}	droplet Sauter diameter, μm
D	diffusion coefficient of benzoic acid in water, m^2s^{-1}
$D(\mathbf{x}, \mathbf{r}, t)$	death function
D_{avg}	average crystal size, m

D_f	fractal dimension
E	expectation value
f	number density function
$g(d')$	breakage kernel, s^{-1}
$g(\boldsymbol{X})$	arbitrary function of vector $\boldsymbol{X}$
G_i	growth rate in i-th dimension
h_1, h_2, h_3	characteristic dimensions of cuboid crystal, m
k_b	kinetic constant, $m^{-3}min^{-1}$
$k_{g,1}, k_{g,2}$	kinetic constants, m/min
K	constant in the aggregation kernel
L_i	length of crystal in i-th dimension, m
m_i	raw moment of the distribution of order i
N	number of cubature points
$\boldsymbol{r}=[r_1, r_2,...,r_N]$	vector of internal coordinates
s	number of phase space dimensions
t	time, s
Tol	cubature tolerance
V_1, V_2	dimensionless volumes of the aggregating particles
V	volume of stirred tank, dm^3
V_{avg}	dimensionless average volume of the population of particles
V_p	dimensionless volume of the particle
v_i	i-th component of the velocity vector in physical space, m/s
w_i	weight of the i-th cubature point
$\boldsymbol{x}=[x_1, x_2, x_3]$	position in the physical space
x_{ij}	j-th coordinate of the i-th abscissa of GC approximation
$\boldsymbol{X}$	s-dimensional vector of random variables

Greek symbols

β	aggregation kernel, m^3/s
$\beta_d(d,d')$	daughter size distribution, m^{-1}
ε	average energy dissipation rate, W/kg
$v(d',\varepsilon)$	number of daughter droplets
ϕ	concentration of the dispersed phase
ρ_c	density of crystal phase, kg/m^3
ρ_s	density of solid phase, kg/m^3
σ	supersaturation
σ_0	initial supersaturation
σ_{in}	supersaturation of the inlet solution
θ	mean residence time, s

Subscripts

$k_1, k_2, ..., k_N$	order of moment over i-th coordinate

Superscript

bs	kinetic exponent
g_1, g_2	kinetic exponent

Abbreviations

DQMOM	direct quadrature method of moment
GC	Gaussian cubature
GQ	Gaussian quadrature
LP	linear program

PB	population balance
PBE	population balance equation
QMOM	quadrature method of moments

REFERENCES

Bałdyga J., Bourne J.R., 1993. Drop breakup and intermittent turbulence. *J. Chem. Eng. Jpn.*, 26, 738-741. DOI: 10.1252/jcej.26.738.

Bałdyga J., Bourne J.R., 1995. Interpretation of turbulent mixing using fractals and multifractals. *Chem. Eng. Sci.*, 50, 381-400. DOI: 10.1016/0009-2509(94)00217-F.

Bałdyga J., Podgórska W., 1998. Drop break-up in intermittent turbulence: maximum stable and transient sizes of drops. *Can. J. Chem. Eng.,* 76, 456-470. DOI: 10.1002/cjce.5450760316.

Batchelor G.K., 1980. Mass transfer from small particles suspended in turbulent fluid. *J. Fluid Mech.,* 98, 609-623. DOI: 10.1017/S0022112080000304.

Borchert C., Nere N., Ramkrishna D., Voigt A., Sundmacher K., 2009. On the prediction of crystal shape distributions in a steady-state continuous crystallizer. *Chem. Eng. Sci.*, 64, 686-696. DOI: 10.1016/j.ces.2008.05.009.

Brändström A., 1966. On the existence of acid salts of monocarboxylic acids in water solutions. *Acta Chem. Scand.,* 20, 1335-1343. DOI: 10.3891/acta.chem.scand.20-1335.

DeVuyst E.A., Preckel P.V, 2007. Gaussian cubature: A practitioner's guide. *Math. Comput. Modell.,* 45, 787–794. DOI: 10.1016/j.mcm.2006.07.021.

Golub G.H., Welsch J.H., 1969. Calculation of Gauss quadrature rules. *Math. Comput. 23*, 221-230. DOI: 10.1090/S0025-5718-69-99647-1.

Gordon R.G., 1968. Error bounds in equilibrium statistical mechanics. *J. Math. Phys. 9*, 655-663. DOI: 10.1063/1.1664624.

Gunawan R., Fusman I., Braatz R.D., 2004. High resolution algorithms for multidimensional population balance equations. *AIChE J.*, 50, 2738-2749. DOI: 10.1002/aic.10228.

Hill P.J., Ng, K.M., 1995. New discretization procedure for the breakage equation. *AIChE J.,* 41, 1204-1216. DOI: 10.1002/aic.690410516.

Hulburt H.M., Katz S., 1964. Some problems in particle technology. A statistical mechanical formulation. *Chem. Eng. Sci.*, 19, 555-574. DOI: 10.1016/0009-2509(64)85047-8.

Marchisio D.L., Fox R.O., 2005. Solution of population balance equations using direct quadrature method of moments. *J. Aerosol Sci.*, 36, 43-73. DOI: 10.1016/j.jaerosci.2004.07.009.

McGraw R., 1997. Description of aerosol dynamics by the quadrature method of moments. *Aerosol Sci. Technol.,* 27, 255-265. DOI: 10.1080/02786829708965471.

Okamoto Y., Nishikawa M., Hashimoto K., 1981. Energy dissipation rate distribution in mixing vessels and its effects on liquid-liquid dispersion and solid-liquid mass transfer. *International Chemical Engineering,* 21, 88-94.

Sack R.A., Donovan A.F., 1972. An algorithm for Gaussian quadrature given modified moments. *Numer. Math.* 18, 465-478. DOI: 10.1007/BF01406683.

Sen M., Chaudhury A., Singh R., Ramachandran R., 2014. Two-dimensional population balance model development and validation of a pharmaceutical crystallization process. *Am. J. Mod. Chem. Eng.*, 1, 13-29.

Silva J.E., Paiva A.P., Soares D., Labrincha A., Castro F., 2007. Crystallization from solution, In *Trends in Hazardous Materials Research.* Nova Science Publishers, New York.

Sorgato, I., 1983. *Statistical approach to kinetics*. Università Degli Studi di Padova- -Istituto di Impianti Chimici, Antoniana S.p.A, Padova, Italy .

Wright D.L., McGraw R., Rosner D.E., 2001. Bivariate extension of the quadrature method of moments for modeling simultaneous coagulation and sintering of particle populations. *J. Colloid Interface Sci.,* 236, 242-251. DOI: 10.1006/jcis.2000.7409.

Received 11 October 2016
Received in revised form 11 July 2017
Accepted 12 July 2017

APPENDIX

The details of application of the GC algorithm to modeling of drop break up with simultaneous mass transfer, as considered in Section 4, are presented in what follows. One starts with choosing internal coordinates, which in this case are the droplet diameter, d_d , and the concentration of the benzoic acid in the dispersed phase, C_d. The bivariate moments of the distribution of order k over droplet diameter and l over the concentration are obtained by transforming Eq. (2):

$$m_{k,l} = \int_0^\infty \int_0^\infty d_d^k C_d^l f\left(d_d, C_d, t\right) dC_d dd_d \tag{30}$$

After performing a moment transformation of the population balance equations, Eq. (3), one gets a set of integro-differential equations governing the time evolution of the system:

$$\begin{aligned} \frac{dm_{k,l}(t)}{dt} = & l\int_0^\infty \int_0^\infty d_d^k C_d^{l-1} \dot{C}_d f\left(d_d, C_d, t\right) dC_d dd_d + \\ & + \int_0^\infty \int_0^\infty \int_{d_d}^\infty d_d^k C_d^l \nu\left(d'_d, \varepsilon\right) \beta_d\left(d_d, d'_d\right) g\left(d'\right) f\left(d'_d, C_d, t\right) dd'_d dC_d dd_d - \\ & - \int_0^\infty \int_0^\infty d_d^k C_d^l g\left(d_d\right) f\left(d_d, C_d, t\right) dC_d dd_d \end{aligned} \tag{31}$$

where $\dot{C}_d$ denotes the mass flux, $\nu(d'_d, \varepsilon)$ the number of daughter droplets created in the breakage event, $\beta_d(d_d, d'_d)$ the daughter size distribution, and $g(d'_d)$ is a breakage kernel. The right hand side terms refer to mass transfer (convection in a phase space), appearing and disappearing of droplets due to breakage (birth and death terms), respectively. The source term integrals are now approximated using the Gaussian Cubature (Eq. (4)) leading to the set of differential equations:

$$\frac{dm_{k,l}(t)}{dt} = l\sum_{i=1}^N d_{di}^k C_{di}^{l-1} \dot{C}_{di} w_i + \sum_{i=1}^N C_{di}^l \left(\nu\left(d_{di}, \varepsilon\right) \int_0^{d_{di}} L^k \beta_d\left(L, d_{di}\right) dL - d_{di}^k \right) g\left(d_{di}\right) w_i \tag{32}$$

To obtain weights, w_i, and abscissas, d_{di} and C_{di}, of the cubature, the GC algorithm is used following Eqs. (5) to (8). One of the output parameters in this case is the Sauter diameter, d_{32}, which requires the second and the third moment of distribution. Hence, the Gaussian cubature of order 3 is used. This order of approximation should ensure sufficient accuracy. Therefore one gets a set of 10 moments of distribution to be followed during the simulation. The linear program (LP) resulting from the GC procedure is then solved in each time step using the dual-simplex method implemented in the MATLAB software libraries giving weights for each point of the previously set up lattice. Points having strictly positive weights are then used for the GC approximation.